MOLECULAR AND CELLULAR BIOLOGY, Nov. 2011, p. 4379–4389 Vol. 31, No. 21
0270-7306/11/$12.00 doi:10.1128/MCB.05854-11

Functional Interplay of the Mre11 Nuclease and Ku in the Response to Replication-Associated DNA Damage▽

Steven S. Foster, Alessia Balestrini, and John H. J. Petrini*

Laboratory of Chromosome Biology, Memorial Sloan-Kettering Cancer Center, New York, New York 10021

Received 23 June 2011/Returned for modification 20 July 2011/Accepted 19 August 2011

The Mre11 complex is a central component of the DNA damage response, with roles in damage sensing, molecular bridging, and end resection. We have previously shown that in *Saccharomyces cerevisiae*, Ku70 (yKu70) deficiency reduces the ionizing radiation sensitivity of *mre11*Δ mutants. In this study, we show that yKu70 deficiency suppressed the camptothecin (CPT) and methyl methanesulfonate (MMS) sensitivity of nuclease-deficient *mre11-3* and *sae2*Δ mutants in an Exo1-dependent manner. CPT-induced G_2/M arrest, γ-H2AX persistence, and chromosome breaks were elevated in *mre11-3* mutants. These outcomes were reduced by yKu70 deficiency. Given that the genotoxic effects of CPT are manifest during DNA replication, these data suggest that Ku limits Exo1-dependent double-strand break (DSB) resection during DNA replication, inhibiting the initial processing steps required for homology-directed repair. We propose that Mre11 nuclease- and Sae2-dependent DNA end processing, which initiates DSB resection prevents Ku from engaging DSBs, thus promoting Exo1-dependent resection. In agreement with this idea, we show that Ku affinity for binding to short single-stranded overhangs is much lower than for blunt DNA ends. Collectively, the data define a nonhomologous end joining (NHEJ)-independent, S-phase-specific function of the Ku heterodimer.

DNA double-strand breaks (DSBs) are repaired via two general mechanisms: nonhomologous end joining (NHEJ) and homology-directed repair (HDR). HDR is initiated through processing and resection of double-stranded DNA (dsDNA) ends to generate 3′ single-stranded DNA (ssDNA) overhangs that ultimately invade homologous duplex DNA, most often a sister chromatid. Recent *in vivo* data suggest a two-step mechanism for DSB resection in mitotic cells. First, 50- to 100-base 3′ ssDNA overhangs are generated by Sae2 and the Mre11 complex, which consists of Mre11, Rad50, and Xrs2. Both Mre11 and Sae2 specify nuclease activities capable of mediating the first incision to generate ssDNA overhangs (31, 54, 64, 66). In the second step, two pathways effect bulk resection: Sgs1, in conjunction with Dna2, and the Exo1 nuclease (17, 42, 72). The *in vitro* requirements for DSB resection are generally consistent with the *in vivo* data (7, 49, 50) although the initial incision step observed *in vivo* is not modeled in the *in vitro* reaction.

Mre11 nuclease activity and Sae2 influence the processing of complex DNA ends. Mre11 nuclease-deficient and *sae2*Δ diploids fail to sporulate due to a defect in the endonucleolytic removal of covalent Spo11 from meiotic DSBs (24, 25, 45, 48). *mre11*Δ, *mre11* nuclease, and *sae2*Δ mutants exhibit sensitivity to camptothecin (CPT) (11, 32, 67), which traps covalent topoisomerase 1 (Top1)-DNA cleavable complexes and induces DNA replication-dependent cell death (15, 19, 56, 59), suggesting that Mre11 and Sae2 may promote the removal of Top1-DNA adducts (11). In addition, *mre11* nuclease and *sae2*Δ mutants are sensitive to high levels of methyl methanesulfonate (MMS) and ionizing radiation (IR) (5, 21, 29, 38, 45), supporting the view that Mre11 and Sae2 may process chemically complex DNA termini to create appropriate substrates for DSB repair enzymes such as those required for DSB resection and ligation.

Additional aspects of Mre11 and Sae2 deficiency support the interpretation that their activities are relevant for the removal of aberrant DNA structures. For example, the Mre11 nuclease and Sae2 cleave hairpin structures *in vivo* and *in vitro* (31, 33, 54, 63, 70). Unlike Mre11, *sae2* alleles separating hairpin opening and Spo11 removal by Sae2 have been identified, suggesting that Sae2 influences more than one activity at complex DNA ends (26). Mre11 nuclease or Sae2 deficiency also confers synthetic lethality with deletion of the gene encoding the Okazaki fragment processing nuclease, Rad27 (10, 45). Though the mechanism of toxicity is unclear, *EXO1* overexpression partially restores *mre11*Δ *rad27*Δ viability (46), suggesting that lethality is associated with a lesion that can be repaired in an Exo1-dependent manner.

We report here that deficiency of budding yeast Ku70 (yKu70), a component of the yKu70-yKu80 heterodimer, which binds DNA ends and hairpins (2, 13, 52), suppresses the CPT and MMS sensitivity of *mre11* nuclease and *sae2*Δ mutants. CPT treatment of *mre11* nuclease mutants induces persistent G_2/M arrest, γ-H2AX signal, chromosome breaks, and hyperrecombination, all of which are reduced by yKu70 deficiency. The *yku70*Δ-dependent rescue requires Exo1, suggesting that yKu70 normally antagonizes a DSB repair process in S-phase cells requiring Mre11 nuclease activity, Sae2, and Exo1. Supporting a role for Ku in S phase, we find that yKu70 deficiency also suppresses the synthetic lethality conferred by Mre11 nuclease and Rad27 deficiency. We show that Ku binds poorly to duplex DNA containing 30-base ssDNA overhangs, such as those created by Mre11 or Sae2, suggesting that the Mre11 nuclease and Sae2 process DSBs to prohibit Ku-mediated inhibition of HDR. Taken together, our data highlight

* Corresponding author. Mailing address: Laboratory of Chromosome Biology, MSKCC, 1275 York Ave., RRL 901C, New York, NY 10021. Phone: (212) 639-2927. Fax: (646) 422-2062. E-mail: petrinij@mskcc.org.

▽ Published ahead of print on 29 August 2011.

TABLE 1. Yeast strains

Strain	Genotype[a]	Source; reference
JPY708	*MAT***a** WT	Petrini laboratory
JPY1216	*MAT***a** *exo1*Δ::*KANMX6*	Petrini laboratory
JPY2252	*MAT***a** *sae2*Δ::*KANMX6*	Petrini laboratory; 26
JPY2258	*MAT*α *sae2*Δ::*HYG*	Petrini laboratory
JPY2421	*MAT***a**/*MAT*α *rad50*Δ/*rad50*Δ *GAL-TEV*/*GAL-TEV ade2-n*/*ade2*–I-SceI *URA3-tetO112 LEU2-TetR-GFP*	Petrini laboratory
JPY3166	*MAT***a** *hta1-S129A hta2-S129A 3×HA-RAD9*::*URA3 ho*Δ *ade3*::*GAL*::*HO bar1*::*ADE3*::*bar1 hml1*::*ADE1 hmr*::*ADE1*	Petrini laboratory
JPY3653	*MAT***a** *yku70*Δ::*KANMX6*	This study
JPY3663	*MAT***a** *mre11-3*::*URA3*	This study
JPY3664	*MAT*α *mre11-3*::*URA3*	This study
JPY4086	*MAT*α *sae2*Δ::*KANMX6 yku70*Δ::*KANMX6*	This study
JPY4087	*MAT***a** *mre11-3*::*URA3 yku70*Δ::*KANMX6*	This study
JPY4115	*MAT*α *mre11-3*::*URA3 dnl4*Δ::*LEU2*	This study
JPY4138	*MAT*α *mre11-3*::*URA3 yku70*Δ::*KANMX6*	This study
JPY4139	*MAT*α *yku70*Δ::*KANMX6*	This study
JPY4140	*MAT***a** *mre11-3*::*URA3 yku70*Δ::*KANMX6*	This study
JPY4141	*mre11-3*::*URA3*	This study
JPY4142	*sgs1*Δ::*TRP1 yku70*Δ::*KANMX6*	This study
JPY4145	*mre11-3*::*URA3 sgs1*Δ::*TRP1 yku70*Δ::*KANMX6*	This study
JPY4150	*yku70*Δ::*KANMX6*	This study
JPY4243	*MAT***a** *rad27*::*KANMX6*	This study
JPY4244	*MAT***a** *mre11-3*::*URA3*	This study
JPY4245	*MAT*α *sgs1*Δ::*TRP1*	This study
JPY4251	*MAT***a** *mre11-3*::*URA3 sgs1*Δ*:TRP1*	This study
JPY4289	*MAT***a** *mre11-3*::*URA3 bar1*Δ::*LEU2*	This study
JPY4290	*MAT***a** *yku70*Δ::*KANMX6 bar1*Δ::*LEU2*	This study
JPY4291	*MAT***a** *bar1*Δ::*LEU2*	This study
JPY4292	*MAT***a** *yku70*Δ::*KANMX6 bar1*Δ::*LEU2*	This study
JPY4294	*MAT***a** *mre11-3*::*URA3 yku70*Δ::*KANMX6 bar1*Δ::*LEU2*	This study
JPY4299	*MAT*α *yku70*Δ::*KANMX6 exo1*Δ::*HIS3*	This study
JPY4300	*MAT***a** *mre11-3*::*URA3 exo1*Δ::*HIS3*	This study
JPY4303	*MAT*α *mre11-3*::*URA3 yku70*Δ::*KANMX6 exo1*Δ::*HIS3*	This study
JPY4311	*MAT***a** *mre11-3*::*URA3 sae2*Δ::*HYG yku70*Δ::*KANMX6*	This study
JPY4316	*MAT***a** *mre11-3*::*URA3 sae2*Δ::*HYG*	This study
JPY4318	*MAT*α *mre11-3*::*URA3 yku70*Δ::*KANMX6*	
JPY4374	*MAT***a** *top1T722A-FLAG3*::*TRP1 bar1*Δ::*LEU2*	This study
JPY4417	*MAT*α *mre11-3*::*URA3 yku70*Δ::*KANMX6 bar1*Δ::*LEU2*	This study
JPY4424	*MAT***a** *mre11-3*::*URA3 yku70*Δ::*KANMX6 bar1*Δ::*LEU2*	This study
JPY4434	*MAT*α *mre11-3*::*URA3*	This study
JPY4660[b]	*MAT***a**/*MAT*α *ade2-n*/*ade2*–I-SceI	This study
JPY4662[b]	*MAT***a**/*MAT*α *ade2-n*/*ade2*–I-SceI *yku70*Δ::*KANMX6*/*yku70*Δ::*KANMX6*	This study
JPY4664[b]	*MAT***a**/*MAT*α *ade2-n*/*ade2*–I-SceI *mre11-3*::*URA3*/*mre11-3*::*URA3*	This study
JPY4665[b]	*MAT***a**/*MAT*α *ade2-n*/*ade2*–I-SceI *mre11-3*::*URA3*/*mre11-3*::*URA3 yku70*Δ::*KANMX6*/*yku70*Δ::*KANMX6*	This study
JPY5181	*MAT***a** *mre11-3*::*URA3 bar1*Δ::*LEU2*	This study
JPY5184	*MAT***a** *mre11-3*::*URA3 yku70*Δ::*KANMX6 bar1*Δ::*LEU2*	This study
JPY5195	*MAT***a** *bar1*Δ::*LEU2*	This study

[a] Strains are in the W303 background (*trp1-1 ura3-1 his3-11,15 leu2-3,112 ade2-1 can1-100 RAD5*).
[b] Strains do not contain *ade2-1*.

two novel findings. First, Mre11 nuclease activity is critical for mitotic DSB repair. Second, by using agents and mutants that induce DSBs in S phase, our experiments support the idea that the Mre11 nuclease and Ku regulate the processing of DNA damage arising during DNA replication and thereby influence the mode by which these lesions are repaired.

MATERIALS AND METHODS

Yeast strains and plasmids. All strains used in this study are in the *Saccharomyces cerevisiae* W303 background (Table 1). Deletions of *YKU70*, *DNL4*, and *EXO1* were generated by standard techniques of PCR-based disruption using pFA vectors (34). To generate *mre11-3* strains (5), full-length *mre11-3*::*URA3* (*mre11-H125L*/*D126V*) was generated by BamHI digestion of pTAP8-*mre11-3*::*URA3* and integrated at the endogenous *MRE11* locus. pRS304-*top1-T722A-FLAG3* was generated by site-directed mutagenesis of pRS304-*TOP1-FLAG3* (contains the 3′ coding region of *TOP1*) (37). The *top1-T722A-FLAG3* strain was generated by integration at the endogenous *TOP1* locus of SpeI-digested pRS304-*top1-T722A-FLAG3*. Plasmid and primer details are available upon request. Haploid strains containing two or more mutations were generated by sporulation and dissection of heterozygous diploids.

DNA damage sensitivity analysis. For spot tests, exponentially growing cultures at 30°C were serially diluted 5-fold and spotted onto solid 1% yeast extract, 2% peptone, and 2% dextrose (YPD) medium containing the drug concentrations indicated on the figures and grown at 30°C for 1 to 2.5 days.

Determination of spore viability. Diploids were sporulated in 1% potassium acetate, pH 7.0, for 3 days at 30°C. Spores were micromanipulated onto YPD medium and grown at 30°C for 3 to 6 days.

Cell cycle and Western blot analysis. G_1-arrested cultures at 2×10^7 cells/ml were split into the required number of smaller cultures and released at 30°C (25°C for flow cytometry) into YPD medium containing the drug doses indicated

in the figure legends. For morphological cell cycle analysis, 5×10^6 cells were fixed at the time points indicated on the figures in 70% ethanol overnight at 4°C. Fixed cells were washed twice in water and sonicated, and the DNA was stained with 4′,6′-diamidino-2-phenylindole (DAPI). The percentage of large-budded mononucleated and binucleated cells was assessed as described previously (65). For analysis by flow cytometry, 1×10^6 fixed cells were incubated in 1 mg/ml RNase at 37°C overnight, followed by 5 mg/ml proteinase K treatment at 50°C for 60 min. Cells were washed once in water, briefly sonicated, resuspended in 10 μM SYTOX Green, and analyzed on a flow cytometer with 488-nm excitation. Flow cytometry data were analyzed using FlowJo. To prepare samples for Western blotting, protein was prepared from 2×10^7 cells by standard trichloroacetic acid (TCA) precipitation. Samples were run on 15% gels and blotted with anti-H2A (phospho-S129A) (15083; Abcam), stripped, and blotted with anti-H2A (39689; Active Motif).

Heteroallelic recombination assay. Diploids heterozygous for the *ade2-n* (20) and *ade2*–I-SceI (47) mutations were grown on YPD medium at 30°C for 4 days. Individual red colonies were diluted in sterile water and plated for single colonies on YPD medium containing dimethyl sulfoxide (DMSO) or 4 μM CPT. Plates were incubated at 30°C for 9 days, and the percentage of colonies containing one or more white sectors was determined. *P* values were calculated using a two-tailed Wilcoxon rank sum test (Mstat software [http://www.mcardle.wisc.edu/mstat/]).

Pulsed-field gel electrophoresis (PFGE). G_1-arrested cultures at 3×10^7 cells/ml were released at 25°C into either DMSO, 50 μM CPT, 0.035% MMS, or 20 μg/ml nocodazole. At the time points indicated on the figures, 1-ml samples were taken, and cell pellets were frozen until required. Agarose plug preparations and electrophoresis were carried out as previously described (36). The gels were stained with 1 μg/ml ethidium bromide overnight and visualized using UV transillumination. Quantitative densitometric analysis was performed using ImageJ. For Southern blotting, DNA was transferred onto Hybond-XL membranes (GE Healthcare) by standard alkaline transfer and blotted with an ARS307 probe. Bands were visualized by a PhosphorImager (Fujifilm).

Band shift assay. All DNA oligonucleotides were obtained from Integrated DNA Technologies (IDT) and PAGE purified before use. The oligonucleotides used to generate the dsDNA substrates with blunt ends (dsBE) (9) or 3′ overhangs (OH) (based on sequence from Burgreev and Mazin [6]) had the following sequences: dsBE-1, GGGTGAACCTGCAGGTGGGCAAAGATGTCCTAGCAATCCATTGGTGATCACTGGTAGCGG; dsBE-2, CCGCTACCAGTGATCACCAATGGATTGCTAGGACATCTTTGCCCACCTGCAGGTTCACCC; 3′ OH-1, ATCAGAGCAGATTGTACTGAGAGTGCACCATATGCGGTGTGAAATACCGCACAGATGCGT; 3′ OH-2, TGGTGCACTCTCAGTACAATCTGCTCTGATCGGCGTATCAATTCGGTCGGGGCTGTGGGC.

dsBE-1 and 3′ OH-1 were labeled at 5′ ends using T4 polynucleotide kinase (NEB). Briefly, 10 pmol of DNA was incubated with 50 U of T4 kinase and 20 μCi of [γ-^{32}P]ATP at 37°C for 1 h. Labeled DNA was purified through a QIAquick kit (Qiagen) according to the manufacturer's instruction. Equimolar amounts of complementary single-stranded DNA oligonucleotides were annealed in a buffer containing 10 mM HEPES (pH 7.5) and 5 mM $MgCl_2$ at 95°C for 1 min, at 65°C for 10 min, at 37°C for 10 min, and at 22°C for 10 min in a PCR Thermocycler. Ku70-Ku80 purified complex (200 pmol) was incubated in the presence of 5′ labeled dsBE (50 fmol) and increasing amounts of unlabeled dsBE or 3′ OH as indicated in Fig. 6A. Binding reactions were carried out in 20 μl of gel retardation buffer (25 mM HEPES-KOH, pH 7.8, 100 mM KCl, 1 mM dithiothreitol [DTT], and 10% glycerol). After incubation at 4°C for 30 min, reaction mixtures were loaded on a 5% neutral polyacrylamide gel prepared in 0.5× Tris-borate-EDTA (TBE) buffer. Gels were run in 0.5× TBE buffer at 70 V for 9 h at 4°C. Labeled DNA products were visualized in the dried gel by a PhosphorImager (Fujifilm) and quantified with the ImageGauge program.

RESULTS

We previously showed that Ku deficiency mitigates the IR sensitivity of *mre11*Δ strains and that the suppressive effect was manifest primarily in S- and G_2-phase cells (4). Based on these observations, we hypothesized that Ku and the Mre11 complex had antagonistic influences on HDR following IR. Loss of Ku has a similar effect on the MMS sensitivity of *rad50*Δ mutants in both budding and fission yeast (61, 68). In this study, given their opposing roles in DSB end resection (30, 42, 72), we examined the effect of yKu70 deficiency in mutants impaired for Mre11-dependent end processing upon challenge with an S phase-specific clastogen, CPT.

***yku70*Δ suppresses *mre11-3* and *sae2*Δ DNA damage sensitivity.** Ku-deficient strains harboring *mre11-3* (nuclease dead) (5) or *sae2*Δ were established. Fivefold serially diluted cultures were plated onto solid medium containing CPT, MMS, or hydroxyurea (HU). *mre11-3* and *sae2*Δ single mutants were sensitive to 10 μM CPT, whereas yKu70-deficient *mre11-3* and *sae2*Δ mutants were resistant up to 30 μM CPT (Fig. 1A). The effect of Ku deficiency observed under conditions of chronic CPT exposure was recapitulated in response to acute treatment (data not shown). Similarly, yKu70 deficiency alleviated the sensitivity of *mre11-3* and *sae2*Δ mutants to 0.015% and 0.02% MMS but conferred a minimal rescue of sensitivity to 125 mM HU (Fig. 1B). These data suggest that the basis of HU sensitivity in *mre11-3* and *sae2*Δ mutants differs from that of CPT and MMS. Supporting this view, yKu70 deficiency did not alter the HU sensitivity of *rad50*Δ mutants but partially alleviated sensitivity to CPT and MMS (data not shown).

That the CPT sensitivity of both *mre11-3* and *sae2*Δ mutants is suppressed by yku70 deficiency suggests that the underlying basis of their respective CPT sensitivities is the same. However, *mre11-3 sae2*Δ double mutants exhibited higher CPT sensitivity than either single mutant (Fig. 1C), raising the possibility that they have nonredundant roles in responding to CPT-induced DNA damage. Nevertheless, deletion of *YKU70* in *mre11-3 sae2*Δ mutants imparted CPT resistance to a similar degree as in either single mutant (Fig. 1C).

Recent reports demonstrate that mutations in DNA ligase IV and Ku mitigate the sensitivity of Fanconi anemia pathway mutants to DNA cross-linking agents, leading to the suggestion that NHEJ of DNA replication-associated lesions compromises cell viability (1, 51). This phenomenon does not underlie the rescue of CPT sensitivity in *mre11-3 yku70*Δ cells as DNA ligase IV deficiency in *mre11-3* mutants did not alter CPT sensitivity at any dose tested (Fig. 1D and data not shown). These data indicate that yKu70 has an NHEJ-independent function that increases the toxicity of CPT-induced DNA lesions.

In the *top1-T722A* mutant, the half-life of the covalent Top1-DNA intermediate is increased, mimicking the effect of CPT (14, 39). Diploid strains harboring *top1-T722A*, *mre11-3*, and *yku70*Δ were generated, and spore viability was assessed. *mre11-3 top1-T722A* double mutant spores were largely inviable, whereas *mre11-3 top1-T722A yku70*Δ triple mutants did not exhibit strong growth defects (Fig. 1E). These data argue that Top1 defects, caused either by chemical or genetic inhibition, lead to the formation of DNA lesions that are substrates for the Mre11 nuclease and Sae2 as well as for yKu70 binding.

In *S. cerevisiae*, CPT treatment results in the accumulation of replication-dependent positive supercoiling in 2-μm circles *in vivo* (28). A similar accumulation of positive supercoiling may be exerted on the chromosomal level, potentially inhibiting replication fork progression. To address the possibility that this effect might partially underlie the CPT sensitivity, we expressed the catalytically active but CPT-resistant Top1-vac protein, which relieves positive supercoiling in yeast (27), in Mre11 nuclease- and Sae2-deficient mutants. Neither *mre11-3* nor *sae2*Δ CPT sensitivity was altered by coexpression of endogenous *S. cerevisiae* Top1 and Top1-vac (data not shown),

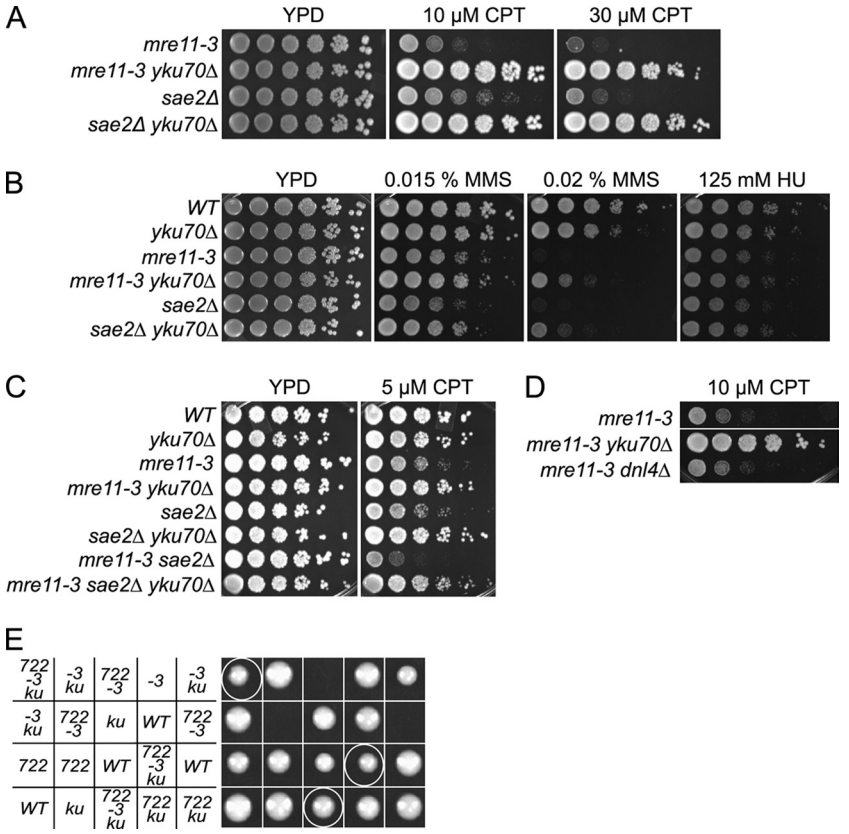

FIG. 1. yKu70 deficiency alleviates the DNA damage sensitivity of *mre11-3* and *sae2*Δ mutants. Growth of *mre11-3* and *sae2*Δ mutants in the absence of yKu70 on CPT (A) and on MMS and HU (B). (C) Growth of *sae2*Δ *mre11-3* mutant on CPT in the absence of yKu70. (D) CPT sensitivity of *mre11-3* mutant in the absence of Dnl4. (E) Genetic interactions between *top1-T722A* (*722*), *mre11-3* (*-3*) and *yku70*Δ (*ku*). Tetrads from a *TOP1*/*top1-T722A MRE11*/*mre11-3 YKU70*/*yku70*Δ sporulated diploid were dissected, and spore viability was assessed by growth.

supporting the view that toxicity was primarily due to DSB induction.

Indices of DNA damage in CPT-treated *mre11-3* cells. We tested the hypothesis that the yield of DSBs in CPT-treated *mre11-3* cells was elevated using several criteria. First, cell cycle progression was assessed. G_1-synchronized cultures were released into 40 μM CPT, and cell cycle position was assessed morphologically. A total of 93% of *mre11-3* cells were scored as large-budded mononucleated cells, indicative of G_2/M arrest, 105 min postrelease into CPT (Fig. 2A, second from left) and remained arrested up to 240 min (data not shown). This prolonged arrest was much less evident in the wild-type (WT), *yku70*Δ, or *mre11-3 yku70*Δ cells. In contrast to *mre11-3*, 55% of CPT-treated WT and 58% of *yku70*Δ cells were binucleated at by 75 and 90 min, respectively, whereas 24% of nuclei in *mre11-3 yku70*Δ mutants were divided at 75 min (Fig. 2A, far right).

Flow cytometric analysis indicated that CPT does not delay S phase and confirmed G_2/M arrest in *mre11-3* cells. It was previously shown that CPT does not induce a notable delay in replication in WT yeast cells (58). Similarly, DMSO- and CPT-treated WT and *mre11-3* cells entered S phase by 20 min and contained diploid DNA content (2n) by 80 min (Fig. 2B). However, consistent with the morphological data, *mre11-3* mutants remained arrested in G_2/M up to 180 min post-G_1 release (data not shown). In contrast, MMS-treated cells exhibited a notable delay within S phase (Fig. 2B), a response that has been shown to result from Mec1-dependent checkpoint activation (55). Given that both MMS and CPT are likely to induce DSBs, the lack of S-phase inhibition in response to CPT treatment may indicate that the checkpoint pathways do not sense the damage induced in *mre11-3* cells until G_2.

A second index of DSB induction was the formation of γ-H2AX. G_1 cultures were released into 40 μM CPT, and γ-H2AX levels at time points following release were determined by Western blotting. As cells entered G_2 (at 45 min, over 80% of cells in late-S/G_2), γ-H2AX signal was detected in all strains (Fig. 2C). The γ-H2AX signal waned in WT, *yku70*Δ, and *mre11-3 yku70*Δ late-G_2 cells (90 min), whereas in *mre11-3* single mutants, signal persisted (Fig. 2C). These data confirm that CPT induces DSB accumulation as cells progress into G_2, and these DSBs persist in *mre11-3* cells, an outcome that is reduced in *mre11-3 yku70*Δ cells.

The third metric of DSB induction applied was the induction of DNA recombination. HDR-directed DSB repair exhibits a strong bias for using the sister chromatid as the repair template (23). We reasoned that if DSBs persisted in CPT-treated diploid *mre11-3* cells, the frequency of inappropriate DSB repair from the homolog would be increased relative to WT cells in which DSBs did not persist. CPT-induced heteroallelic recombination was scored using diploid strains heterozygous for the *ade2-n* and *ade2*–I-SceI alleles. As a result of Ade2 deficiency,

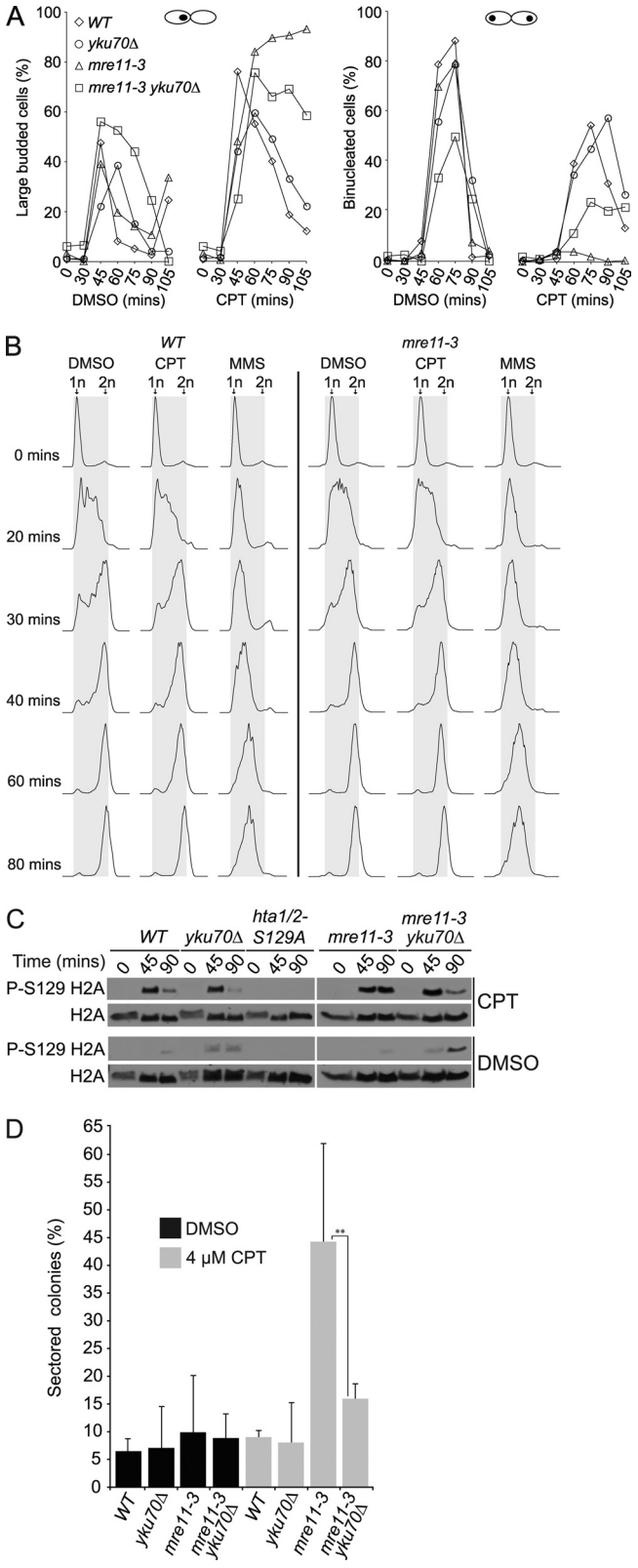

FIG. 2. CPT treatment induces G_2/M arrest, γ-H2AX, and heteroallelic recombination in *mre11-3* mutants. G_1-arrested (0 min) cultures of the indicated strains were released into YPD medium containing DMSO, 40 μM CPT, or 0.035% MMS. (A) Cell cycle stage was determined by counting large-budded mononucleated (left-hand panels) and binucleated (right-hand panels) cells. (B) S-phase progression analyzed by flow cytometry. Experiments were each repeated three times. Representative data from single experiments are shown. (C) CPT-dependent γ-H2AX signal was determined in the indicated mutants by Western blotting. *hta1/2-S129A* indicates the H2A phosphorylation site mutant; P-S129 H2A indicates H2A-S129 phosphorylation. (D) Gene conversion in diploids heterozygous for the *ade2-n* and *ade2–I-SceI* mutations and harboring the indicated mutations. Heteroallelic recombination was assessed by determining the percentage of red colonies containing one or more white sectors. Data shown represent averages from four biological replicates. Error bars represent standard deviation ($P = 0.0039$).

these strains grow as red colonies, and heteroallelic recombination leads to white sectoring (20).

Red colonies from WT, *yku70*Δ, *mre11-3*, and *mre11-3 yku70*Δ diploids heterozygous for the *ade2* mutations were replated onto YPD plates containing either DMSO or 4 μM CPT. Induction of sectoring was negligible in WT and *yku70*Δ mutants. Growth on CPT increased the frequency of heteroallelic recombination in *mre11-3* mutants 4.5-fold relative to DMSO-treated controls, whereas *mre11-3 yku70*Δ mutants exhibited only a 1.8-fold increase in CPT-induced recombination (Fig. 2D). A similar trend was observed at 2 μM CPT on synthetic complete medium (data not shown).

Finally, the effects of CPT were monitored by PFGE. With this technique, DSBs result in the diminution of full-length chromosome bands and the appearance of smears. In addition, replication intermediates are unable to enter the gel under the conditions used, providing a gross assessment of replication fork abundance at a given time point. Cells were released from G_1 arrest into 50 μM CPT and harvested, and chromosomes were resolved by PFGE, with G_1-arrested (n) and G_2-arrested (2n) cultures serving as controls. At 25 min post-G_1 release, the abundance of intact chromosomes in WT and *mre11-3* cells was reduced irrespective of CPT treatment (Fig. 3A, lanes 3, 5, 10, and 12), consistent with the bulk of the cultures entering S phase (Fig. 3B). By 75 min, chromosome band intensities in DMSO-treated cultures approximated those of nocodazole-arrested G_2 cells (Fig. 3A, lanes 2, 4, and 11). Chromosome band intensities in CPT-treated cultures did not recover by 75 min. The single band attributable to chromosomes VII and XV exhibited approximately 63% and 31% of the signal intensity relative to the corresponding DMSO band in WT and *mre11-3* cells, respectively (Fig. 3A, lanes 4, 6, 11, and 13). However, by 90 min, chromosome band intensities were similar between DMSO- and CPT-treated WT G_2 cultures (data not shown). In contrast, the intensity of chromosomal bands in CPT-treated *mre11-3* cells did not recover to the level of G_2 cells, and extensive smearing was evident (Fig. 3A, lane 6, and C, lanes 6 and 7). The smearing observed was markedly reduced in *mre11-3 yku70*Δ cells (Fig. 3C, lanes 13 and 14), and band intensities were indistinguishable between DMSO- and CPT-treated cultures (Fig. 3C, lanes 11 and 14).

Unlike CPT treatment, MMS caused the accumulation of cells in S phase (Fig. 3B), with virtually all of the chromosomes blocked from entering the gel by 75 min (Fig. 3A, lanes 8 and 15). Nevertheless, the possibility that CPT-treated *mre11-3* cells had blocked replication intermediates in addition to DSBs was addressed. Southern blotting with a probe specific to chro-

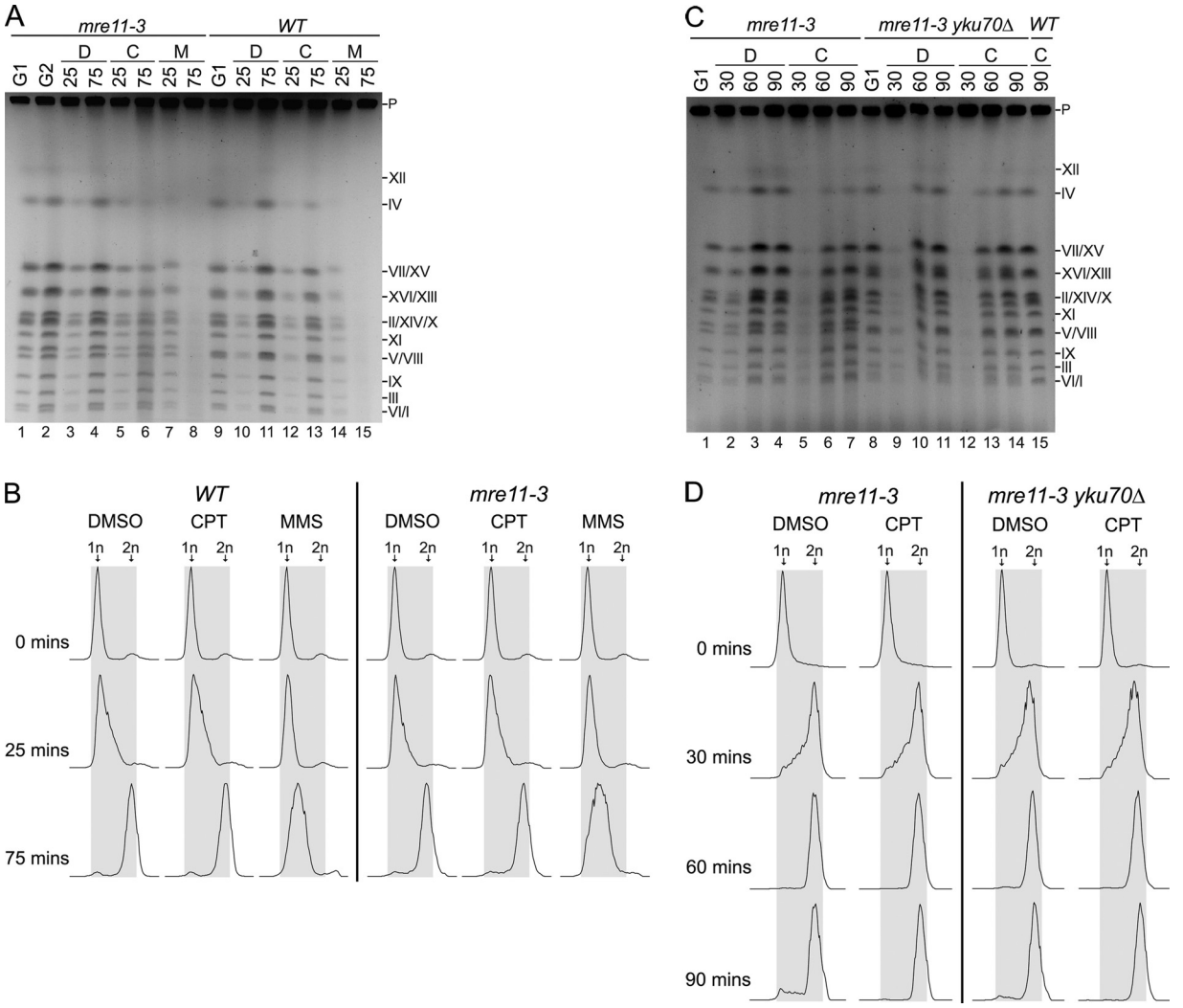

FIG. 3. CPT induces chromosome breakage in *mre11-3* mutants. Chromosome integrity was monitored by PFGE analysis. (A) Analysis of WT and *mre11-3* cells. G_1-arrested cells were released into DMSO (D), 50 μM CPT (C), or 0.035% MMS (M). Numbers above the gel indicate time (in min) post-G_1 release; P indicates plug; lane numbers appear below the gel. G_1 (alpha-factor arrested) and G_2 (nocodazole arrested) cells indicate 1n and 2n DNA controls, respectively. The ethidium bromide-stained gel was visualized using UV transillumination. A single representative gel is shown. Observations were confirmed with independent strains. (B) Cell cycle analysis of samples used in panel A. (C) Analysis of *mre11-3* and *mre11-3 yku70*Δ cultures. (D) Cell cycle analysis of samples used in panel C.

mosome III was carried out to detect persistent non-DSB complex DNA structures in CPT-arrested *mre11-3* cells, which we reasoned would remain in the plug or migrate more slowly. The data obtained were consistent with the presence of lower-molecular-weight DNA, and the presence of aberrant DNA structures was not indicated in *mre11-3* samples (data not shown). DSB formation, as inferred from PFGE, was not dependent upon Mus81 as *mre11-3 mus81*Δ mutants were indistinguishable from *mre11-3* cells in that experimental setting (data not shown). Collectively, these data support the view that CPT induces DSBs in *mre11-3* mutants although we cannot exclude the possibility that non-DSB structures also contribute to the phenotypes observed.

Exo1 is required for *yku70*Δ-dependent suppression of CPT sensitivity. Given that yKu70 deficiency increases ssDNA generation at HO-induced DSBs and telomeres (30, 35), we hypothesized the *yku70*Δ-mediated rescue of Mre11 nuclease deficiency was attributable to increased resection of DSBs leading to the generation of substrates suitable for HDR. To test this, we assessed the requirement of Exo1 and Sgs1 in *yku70*Δ-dependent CPT resistance.

We found that Exo1 deficiency abolished *yku70*Δ-dependent suppression of *mre11-3* CPT sensitivity (Fig. 4A). *mre11-3 exo1*Δ *yku70*Δ triple mutants exhibited a higher CPT sensitivity than either *mre11-3 yku70*Δ or *mre11-3* cells. In addition, Exo1 deficiency partially increased the CPT sensitivity of both *mre11-3* and *yku70*Δ single mutants, supporting the view that DNA end resection by Exo1 is the basis of the *yku70*Δ rescue (Fig. 4A). A similar phenotype was observed in fission yeast (69). These data are consistent with the view that Ku inhibits the ability of Exo1 to act at DSB ends.

Like Exo1, Sgs1 functions in the later stages of DSB resec-

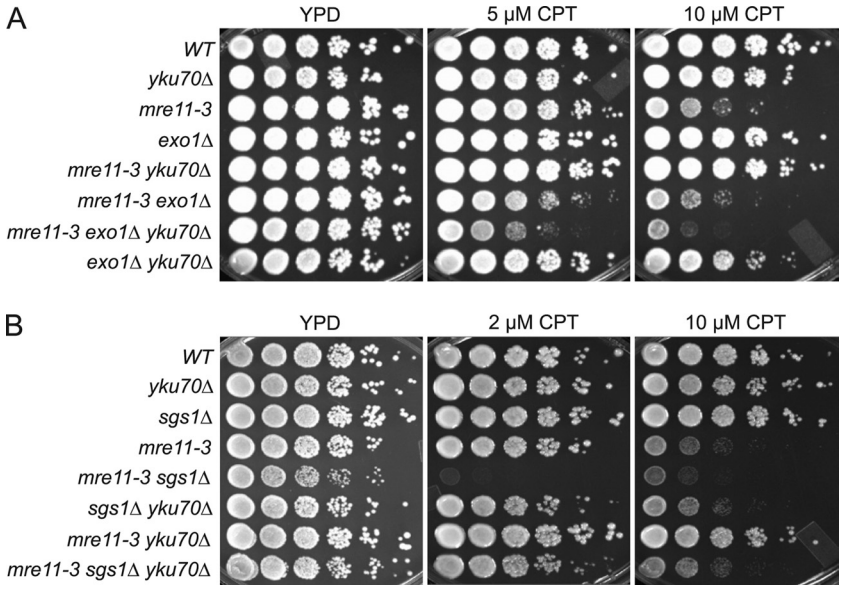

FIG. 4. The *yku70*Δ-dependent rescue of *mre11-3* CPT sensitivity requires *EXO1.* CPT sensitivity of *mre11-3 yku70*Δ mutants in the absence of Exo1 (A) and Sgs1 (B).

tion (17, 42, 72); however, deletion of Sgs1 did not phenocopy *exo1*Δ. *mre11-3 sgs1*Δ and *yku70*Δ *sgs1*Δ cells exhibited sharply increased CPT sensitivity relative to *mre11-3* and *yku70*Δ cells, respectively (Fig. 4B). Deletion of Ku to create *mre11-3 sgs1*Δ *yku70*Δ triple mutants increased CPT resistance relative to *mre11-3 sgs1*Δ double mutants, approximately to the level of *sgs1*Δ *yku70*Δ at 2 μM and 10 μM CPT. Given its antirecombinogenic role (16, 22), the CPT hypersensitivity of *mre11-3 sgs1*Δ and *yku70*Δ *sgs1*Δ mutants may be attributable to the accumulation of CPT-induced toxic recombination intermediates. Alternatively, the synergistic CPT sensitivity of *mre11-3 sgs1*Δ mutants may reflect additivity of their resection defects.

***mre11-3 rad27*Δ synthetic lethality is suppressed by yKu70 deficiency.** Nuclease-deficient *mre11* mutants are synthetically lethal with *rad27*Δ (10, 45). *rad27*Δ strains exhibit a dramatic increase in gross chromosomal rearrangements (8), indicating that spontaneous chromosome breakage is elevated in those cells, presumably as a result of replication fork breakage. To test the hypothesis that synthetic lethality is attributable to defects in the repair of replication associated DSBs, *MRE11*/*mre11-3 RAD27*/*rad27*Δ *YKU70*/*yku70*Δ diploids were sporulated, and viability was assessed. As expected, all *mre11-3 rad27*Δ double mutants were inviable, but in the context of yKu70 deficiency, 14 out of 17 *mre11-3 rad27*Δ *yku70*Δ spores grew into a visible colony (Fig. 5). Spore viability in this context was not due to perdurance of the proteins from the heterozygous parents, as restreaks of the triple mutants remain viable (data not shown). Similarly, yKu70 deficiency was recently shown to alleviate the growth defect in *sae2*Δ *rad27*Δ mutants (41). These data support the interpretation that the *mre11-3 rad27*Δ synthetic lethality is attributable to the accumulation of a toxic DNA structure that would otherwise be engaged by Ku. Given that Exo1 overexpression also suppresses this synthetic lethality, a parsimonious interpretation would be that the toxic structure in question is a DSB. As with CPT-associated DSBs, suppression of this *mre11-3* phenotype by yKu70 deficiency reflects an S-phase-specific, NHEJ-independent function of the Ku heterodimer.

Ku binds poorly to ssDNA overhangs. The data presented thus far indicated that yKu70 inhibited DSB repair in the absence of the Mre11 nuclease and Sae2 and led us to suggest that the generation of short ssDNA overhangs by the Mre11 nuclease and Sae2 is required to inhibit Ku binding at DSB ends, thereby priming ends for Exo1-dependent long-range resection and HDR. Alternatively, given its high affinity for DNA ends, Ku may rapidly bind at DSBs prior to end processing by Mre11/Sae2. This scenario would suggest that the Mre11

-3 ku	*ku*	*ku*	*-3 ku*	*ku*	*-3 27 ku*	*WT*	*27*	*ku*
27	*-3 27 ku*	*-3 27 ku*	*27 ku*	*-3 27 ku*	*-3 ku*	*27*	*-3 27 ku*	*-3 ku*
27	*-3 27*	*27*	*-3 27 ku*	*27*	*WT*	*-3 27 ku*	*-3 ku*	*27*
-3 ku	*WT*	*-3*	*WT*	*-3*	*27*	*-3 ku*	*WT*	*-3 27*

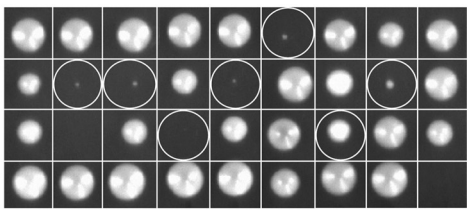

FIG. 5. yKu70 deficiency alleviates the *mre11-3 rad27*Δ synthetic lethality. Genetic interactions between *mre11-3* (*-3*), *rad27*Δ (*27*), and *yku70*Δ (*ku*). Tetrads from an *MRE11*/*mre11-3 RAD27*/*rad27*Δ *yku70*Δ/*YKU70* sporulated diploid were dissected, and spore viability was assessed by growth.

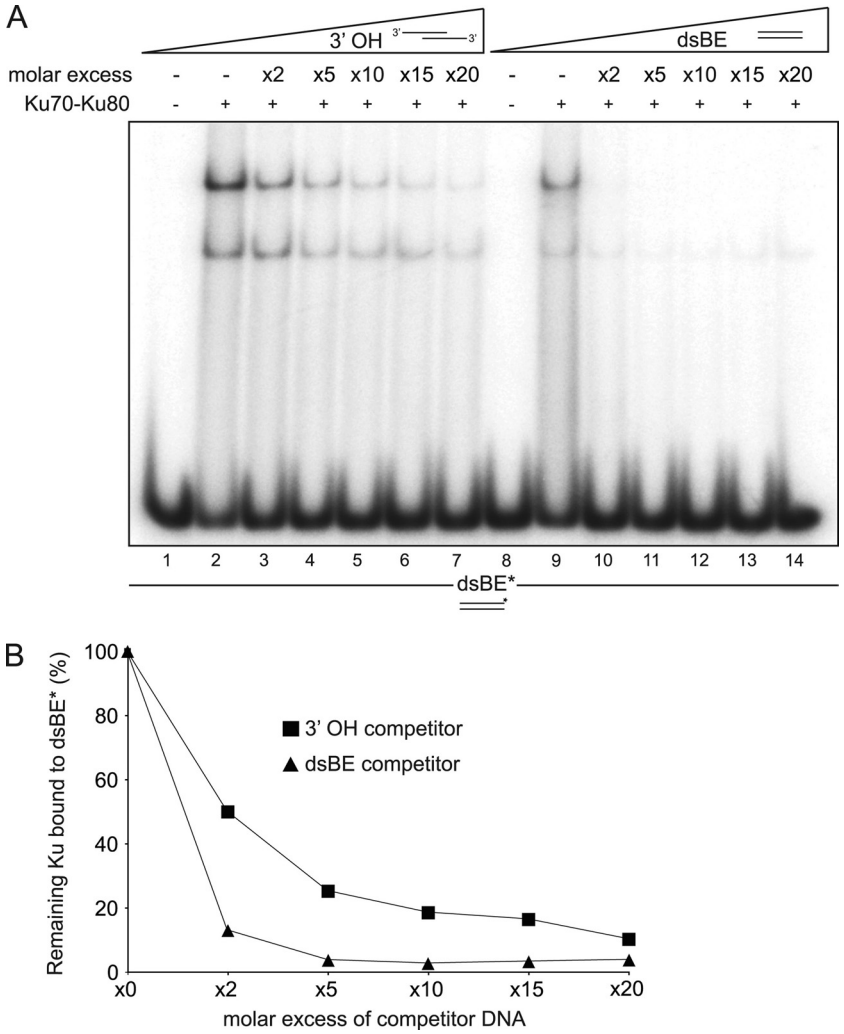

FIG. 6. Ku preferentially binds blunt DNA ends over short ssDNA overhangs. (A) Ku70-Ku80 purified complex (200 pmol) was incubated with 50 fmol of 5′ labeled dsDNA (dsBE*, 60 bp of dsDNA with blunts ends) and increasing amounts of unlabeled dsBE DNA or a substrate containing 30 bp of dsDNA with 30-base 3′ overhangs (3′ OH). Lane numbers are indicated below the gel. (B) Quantification of gel in panel A. The experiment was repeated three times with similar results.

nuclease and Sae2 endonucleolytically clip DSBs to remove already bound Ku.

We tested the ability of Ku to bind ssDNA overhang ends analogous to those generated by Mre11/Sae2 using electrophoretic mobility shift assays. Incubation of Ku complex with a radioactively labeled 60-bp blunt-ended dsDNA substrate produced slowly migrating species (Fig. 6A, lanes 2 and 9), reflecting Ku's previously established DNA end binding function (3, 53). Addition of cold blunt-ended DNA prior to binding markedly reduced the abundance of the shifted species (Fig. 6A, lanes 10 to 14), resulting in a 27-fold decrease of labeled Ku-DNA complex when present at five times molar excess (Fig. 6B). In contrast, a five times molar excess of unlabeled duplex DNA containing 30-base overhangs diminished the shifted product by only 4-fold (Fig. 6A, lanes 3 to 7, and B). These data demonstrate that, relative to blunt ends, Ku binds poorly to DNA ends containing ssDNA overhangs, supporting the hypothesis that Mre11 nuclease- and Sae2-dependent processing of DSBs *in vivo* discourages engagement by the Ku heterodimer and promotes DSB resection.

DISCUSSION

In this study we investigated the interplay of Mre11 and Sae2, both required for early steps in the processing of DNA ends prior to DNA repair, and the DNA end binding factor yKu70. The data herein demonstrate a critical role for Mre11 nuclease activity in the repair of replication-dependent DSBs and highlight an NHEJ-independent role for yKu70 in antagonizing DSB repair in S phase and G_2.

We show that Mre11 nuclease activity and Sae2 are largely dispensable for cell viability in yKu70-deficient cells while the requirement for Exo1 remains. On this basis, we propose that Ku binds to and excludes Exo1 from processing DNA structures that are formed in response to CPT-induced genotoxic stress. Given that Mre11 and Sae2 act upstream of Exo1 in

DSB end resection (42, 72), we propose that initial endonucleolytic cleavage events are catalyzed by the Mre11 nuclease and Sae2 and serve to inhibit Ku binding, thereby potentiating Exo1-mediated resection and promoting HDR-dependent repair.

The model proposed above posits that Ku deficiency facilitates the resolution of toxic DNA adducts stabilized by Mre11 nuclease and Sae2 deficiency. Implicitly, this hypothesis requires that the DNA structures to which Ku binds are normally processed by the Mre11 nuclease and Sae2 and are thus more abundant in Mre11 nuclease- and Sae2-deficient cells.

Several lines of evidence support the view that these toxic DNA structures are DSBs. First, Ku exhibits a strong preference for binding to dsDNA ends over ssDNA or circular DNA (12, 43, 53). Second, CPT-induced cell cycle arrest, γ-H2AX signal, heteroallelic recombination, and chromosome breakage were all enhanced in *mre11-3* cells and reduced to essentially wild-type levels in *mre11-3 yku70*Δ double mutant cells (Fig. 2 and 3). These endpoints are each sensitive indices of DSB abundance and support the interpretation that yKu70 antagonizes HDR-mediated DSB repair in S phase and G_2 in the absence of Mre11 nuclease activity. The function of Ku in this regard is not simply to promote NHEJ over HDR as inactivating NHEJ via a DNA ligase IV deficiency had no effect on *mre11-3* CPT sensitivity (Fig. 1D). These and other data support the view that DSB end binding by the Ku heterodimer influences mitotic DNA repair by limiting access of Exo1 for resection.

We propose that a role of the initial cleavage step at mitotic DSB ends by the Mre11 nuclease and Sae2 is to counterbalance this NHEJ-independent Ku function though the precise interaction between Mre11 and Sae2 during end processing remains unclear. In light of their role in this mechanism, the clastogen sensitivities observed in Mre11 nuclease and Sae2 deficiency are likely attributable to defects in HDR-mediated DNA repair. In this model, the initial Mre11 nuclease/Sae2-dependent cleavage step would inhibit or dismantle Ku binding at DSB ends and thereby promote resection by Exo1. Consistent with this view, Ku has a significantly higher affinity for blunt dsDNA ends over short ssDNA overhangs (Fig. 6). Accordingly, Ku deficiency effectively bypasses the need for the initial incision step and permits Exo1 to effect resection in *mre11-3* and *sae2*Δ mutants. In further support of this idea, Ku deficiency was recently shown to alleviate the resection defect at an HO-induced DSB in *rad50*Δ and *sae2*Δ mutants (41, 60). On the other hand, *mre11-3* and *sae2*Δ mutants, unlike *mre11*Δ cells, did not exhibit higher detectable levels of Ku bound at an HO-induced DSB when measured by chromatin immunoprecipitation (ChIP) (60, 71). This discrepancy may be attributable to differential processing requirements of HO- and CPT-induced DNA ends and additionally due to the S-phase specificity of CPT-induced lesions.

We consider two nonexclusive possibilities for the molecular basis of increased DSBs in CPT-treated *mre11-3* mutants: defects in the resolution of topoisomerase adducts and defects in DSB repair. Several lines of evidence support the view that both the Mre11 complex and Sae2 promote the resolution of Top1-DNA cleavage complexes. Impaired resolution would increase the stability of adducts and accordingly increase the risk of collision with the replisome. Increased levels of Top1-DNA adducts have been detected in *Schizosaccharomyces pombe rad32^{mre11}-D65N* nuclease and *rad50S* mutants (18), and *S. cerevisiae mre11* and *sae2*Δ mutants and murine *Rad50$^{S/S}$* cells are CPT sensitive (Fig. 1A) (11, 44). It is conceivable that the Ku heterodimer may bind to Top1-associated DSB ends. However, the flap endonuclease activity of Exo1 is the incorrect polarity to remove the Top1-associated ends (62). Hence, this could not account for the suppression of CPT sensitivity by yKu70 deficiency in *mre11-3* and *sae2*Δ cells.

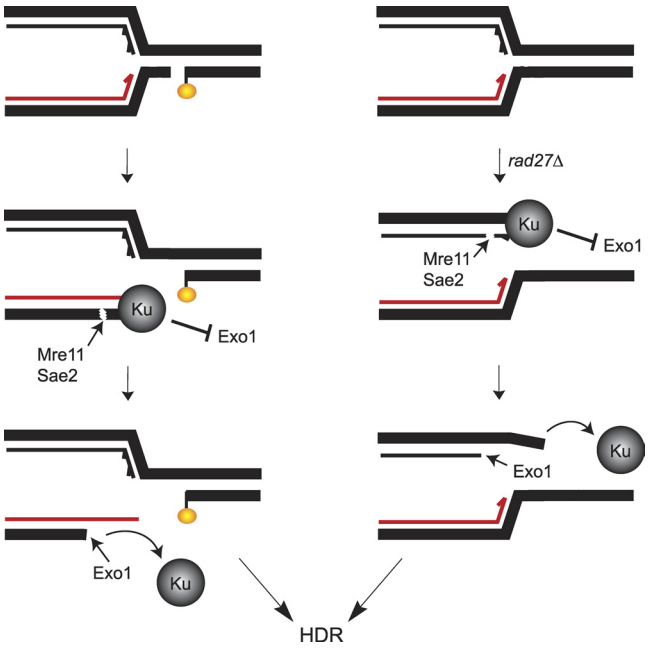

FIG. 7. Antagonistic roles for Ku and Mre11 in S-phase DSB metabolism. We propose that the resection of DNA replication-associated DSBs is regulated negatively by the Ku heterodimer and positively by Mre11 nuclease- or Sae2-dependent activities. In this figure, DSBs associated with CPT lesions are depicted on the left, and those associated with fork breakage in *rad27*Δ are shown on the right. In both cases, the action of Mre11 or Sae2 ultimately promotes resection, potentiating HDR of the DSB.

An alternative scenario is that the leading strand encounters the 5′ OH side of the nick created by the cleavage complex, leading to polymerase runoff and ultimately a single-ended DSB (57). These DSB ends would likely be substrates for Mre11 and Sae2, as well as Ku binding. These DSBs would accumulate in *mre11-3* cells in a Ku-dependent, Mus81-independent manner and are possibly the basis of the *mre11-3* CPT toxicity (Fig. 7). In this scenario, the Exo1-dependent suppression of *mre11-3* CPT sensitivity by *yku70*Δ would reflect the promotion of DSB resection en route to HDR-mediated repair (Fig. 7).

Finally, a competitive relationship between Ku and the Mre11 complex has been suggested to provide a mechanism of DSB processing and repair pathway choice (41, 60, 61, 71). Limited resection in G_1 cells promotes Ku- and DNA ligase IV-dependent NHEJ, whereas increased cyclin-dependent kinase (CDK) activity leads to increased resection and promotion of HDR (40). However, the data presented herein clearly demonstrate a previously uncharacterized role for Ku in mediating DSB repair during DNA replication and the subse-

quent G_2. The S/G_2 functions of Ku are independent of NHEJ and suggest that the heterodimer exerts a relatively broad regulatory influence on the metabolism of toxic DNA structures formed in the course of DNA replication.

ACKNOWLEDGMENTS

We thank Lorraine Symington for the *ade2-n* and *ade2*–I-SceI mutants, Alain Verreault for pRS-*TOP1-FLAG3* vectors, Mary-Ann Bjornsti for YCp-*ScTop1* vectors, Xiaolan Zhao for the *mus81*Δ mutant and advice, Alan Tomkinson for Ku protein, Marco Muzi-Falconi for anti-Rad53, Stewart Shuman for advice, and Marcel Hohl and other members of our laboratory for insightful discussion. We are particularly indebted to Massimo Lopes and Arnab Ray Chaudhuri for advice on this study.

This work was supported by the American Italian Cancer Foundation (A.B.) and NIH grants to J.H.J.P.

REFERENCES

1. **Adamo, A., et al.** 2010. Preventing nonhomologous end joining suppresses DNA repair defects of Fanconi anemia. Mol. Cell **39:**25–35.
2. **Arosio, D., et al.** 2002. Studies on the mode of Ku interaction with DNA. J. Biol. Chem. **277:**9741–9748.
3. **Bianchi, A., and T. de Lange.** 1999. Ku binds telomeric DNA *in vitro*. J. Biol. Chem. **274:**21223–21227.
4. **Bressan, D. A., B. K. Baxter, and J. H. Petrini.** 1999. The Mre11-Rad50-Xrs2 protein complex facilitates homologous recombination-based double-strand break repair in *Saccharomyces cerevisiae*. Mol. Cell. Biol. **19:**7681–7687.
5. **Bressan, D. A., H. A. Olivares, B. E. Nelms, and J. H. Petrini.** 1998. Alteration of N-terminal phosphoesterase signature motifs inactivates *Saccharomyces cerevisiae* Mre11. Genetics **150:**591–600.
6. **Bugreev, D. V., and A. V. Mazin.** 2004. Ca2+ activates human homologous recombination protein Rad51 by modulating its ATPase activity. Proc. Natl. Acad. Sci. U. S. A. **101:**9988–9993.
7. **Cejka, P., et al.** 2010. DNA end resection by Dna2-Sgs1-RPA and its stimulation by Top3-Rmi1 and Mre11-Rad50-Xrs2. Nature **467:**112–116.
8. **Chen, C., and R. D. Kolodner.** 1999. Gross chromosomal rearrangements in *Saccharomyces cerevisiae* replication and recombination defective mutants. Nat. Genet. **23:**81–85.
9. **Ciccia, A., et al.** 2007. Identification of FAAP24, a Fanconi anemia core complex protein that interacts with FANCM. Mol. Cell **25:**331–343.
10. **Debrauwere, H., S. Loeillet, W. Lin, J. Lopes, and A. Nicolas.** 2001. Links between replication and recombination in *Saccharomyces cerevisiae*: a hypersensitive requirement for homologous recombination in the absence of Rad27 activity. Proc. Natl. Acad. Sci. U. S. A. **98:**8263–8269.
11. **Deng, C., J. A. Brown, D. You, and J. M. Brown.** 2005. Multiple endonucleases function to repair covalent topoisomerase I complexes in *Saccharomyces cerevisiae*. Genetics **170:**591–600.
12. **Dynan, W. S., and S. Yoo.** 1998. Interaction of Ku protein and DNA-dependent protein kinase catalytic subunit with nucleic acids. Nucleic Acids Res. **26:**1551–1559.
13. **Feldmann, H., and E. L. Winnacker.** 1993. A putative homologue of the human autoantigen Ku from *Saccharomyces cerevisiae*. J. Biol. Chem. **268:** 12895–12900.
14. **Fiorani, P., and M. A. Bjornsti.** 2000. Mechanisms of DNA topoisomerase I-induced cell killing in the yeast *Saccharomyces cerevisiae*. Ann. N. Y. Acad. Sci. **922:**65–75.
15. **Furuta, T., et al.** 2003. Phosphorylation of histone H2AX and activation of Mre11, Rad50, and Nbs1 in response to replication-dependent DNA double-strand breaks induced by mammalian DNA topoisomerase I cleavage complexes. J. Biol. Chem. **278:**20303–20312.
16. **Gangloff, S., C. Soustelle, and F. Fabre.** 2000. Homologous recombination is responsible for cell death in the absence of the Sgs1 and Srs2 helicases. Nat. Genet. **25:**192–194.
17. **Gravel, S., J. R. Chapman, C. Magill, and S. P. Jackson.** 2008. DNA helicases Sgs1 and BLM promote DNA double-strand break resection. Genes Dev. **22:**2767–2772.
18. **Hartsuiker, E., M. J. Neale, and A. M. Carr.** 2009. Distinct requirements for the Rad32(Mre11) nuclease and Ctp1(CtIP) in the removal of covalently bound topoisomerase I and II from DNA. Mol. Cell **33:**117–123.
19. **Hsiang, Y. H., M. G. Lihou, and L. F. Liu.** 1989. Arrest of replication forks by drug-stabilized topoisomerase I-DNA cleavable complexes as a mechanism of cell killing by camptothecin. Cancer Res. **49:**5077–5082.
20. **Huang, K. N., and L. S. Symington.** 1994. Mutation of the gene encoding protein kinase C 1 stimulates mitotic recombination in *Saccharomyces cerevisiae*. Mol. Cell. Biol. **14:**6039–6045.
21. **Huertas, P., F. Cortes-Ledesma, A. A. Sartori, A. Aguilera, and S. P. Jackson.** 2008. CDK targets Sae2 to control DNA-end resection and homologous recombination. Nature **455:**689–692.
22. **Ira, G., A. Malkova, G. Liberi, M. Foiani, and J. E. Haber.** 2003. Srs2 and Sgs1-Top3 suppress crossovers during double-strand break repair in yeast. Cell **115:**401–411.
23. **Kadyk, L. C., and L. H. Hartwell.** 1992. Sister chromatids are preferred over homologs as substrates for recombinational repair in *Saccharomyces cerevisiae*. Genetics **132:**387–402.
24. **Keeney, S., C. N. Giroux, and N. Kleckner.** 1997. Meiosis-specific DNA double-strand breaks are catalyzed by Spo11, a member of a widely conserved protein family. Cell **88:**375–384.
25. **Keeney, S., and N. Kleckner.** 1995. Covalent protein-DNA complexes at the 5′ strand termini of meiosis-specific double-strand breaks in yeast. Proc. Natl. Acad. Sci. U. S. A. **92:**11274–11278.
26. **Kim, H. S., et al.** 2008. Functional interactions between Sae2 and the Mre11 complex. Genetics **178:**711–723.
27. **Knab, A. M., J. Fertala, and M. A. Bjornsti.** 1993. Mechanisms of camptothecin resistance in yeast DNA topoisomerase I mutants. J. Biol. Chem. **268:**22322–22330.
28. **Koster, D. A., K. Palle, E. S. Bot, M. A. Bjornsti, and N. H. Dekker.** 2007. Antitumour drugs impede DNA uncoiling by topoisomerase I. Nature **448:** 213–217.
29. **Lee, S. E., D. A. Bressan, J. H. Petrini, and J. E. Haber.** 2002. Complementation between N-terminal *Saccharomyces cerevisiae mre11* alleles in DNA repair and telomere length maintenance. DNA Repair (Amst.) **1:**27–40.
30. **Lee, S. E., et al.** 1998. *Saccharomyces* Ku70, Mre11/Rad50, and RPA proteins regulate adaptation to G_2/M arrest after DNA damage. Cell **94:**399–409.
31. **Lengsfeld, B. M., A. J. Rattray, V. Bhaskara, R. Ghirlando, and T. T. Paull.** 2007. Sae2 is an endonuclease that processes hairpin DNA cooperatively with the Mre11/Rad50/Xrs2 complex. Mol. Cell **28:**638–651.
32. **Liu, C., J. J. Pouliot, and H. A. Nash.** 2002. Repair of topoisomerase I covalent complexes in the absence of the tyrosyl-DNA phosphodiesterase Tdp1. Proc. Natl. Acad. Sci. **99:**14970–14975.
33. **Lobachev, K. S., D. A. Gordenin, and M. A. Resnick.** 2002. The Mre11 complex is required for repair of hairpin-capped double-strand breaks and prevention of chromosome rearrangements. Cell **108:**183–193.
34. **Longtine, M. S., et al.** 1998. Additional modules for versatile and economical PCR-based gene deletion and modification in *Saccharomyces cerevisiae*. Yeast **14:**953–961.
35. **Maringele, L., and D. Lydall.** 2002. *EXO1*-dependent single-stranded DNA at telomeres activates subsets of DNA damage and spindle checkpoint pathways in budding yeast *yku70*Δ mutants. Genes Dev. **16:**1919–1933.
36. **Maringele, L., and D. Lydall.** 2006. Pulsed-field gel electrophoresis of budding yeast chromosomes. Methods Mol. Biol. **313:**65–73.
37. **Masumoto, H., D. Hawke, R. Kobayashi, and A. Verreault.** 2005. A role for cell-cycle-regulated histone H3 lysine 56 acetylation in the DNA damage response. Nature **436:**294–298.
38. **McKee, A. H., and N. Kleckner.** 1997. A general method for identifying recessive diploid-specific mutations in *Saccharomyces cerevisiae*, its application to the isolation of mutants blocked at intermediate stages of meiotic prophase and characterization of a new gene SAE2. Genetics **146:**797–816.
39. **Megonigal, M. D., J. Fertala, and M. A. Bjornsti.** 1997. Alterations in the catalytic activity of yeast DNA topoisomerase I result in cell cycle arrest and cell death. J. Biol. Chem. **272:**12801–12808.
40. **Mimitou, E. P., and L. S. Symington.** 2009. DNA end resection: many nucleases make light work. DNA Repair (Amst.) **8:**983–995.
41. **Mimitou, E. P., and L. S. Symington.** 2010. Ku prevents Exo1 and Sgs1-dependent resection of DNA ends in the absence of a functional MRX complex or Sae2. EMBO J. **29:**3358–3369.
42. **Mimitou, E. P., and L. S. Symington.** 2008. Sae2, Exo1 and Sgs1 collaborate in DNA double-strand break processing. Nature **455:**770–774.
43. **Mimori, T., and J. A. Hardin.** 1986. Mechanism of interaction between Ku protein and DNA. J. Biol. Chem. **261:**10375–10379.
44. **Morales, M., et al.** 2008. DNA damage signaling in hematopoietic cells: a role for Mre11 complex repair of topoisomerase lesions. Cancer Res. **68:** 2186–2193.
45. **Moreau, S., J. R. Ferguson, and L. S. Symington.** 1999. The nuclease activity of Mre11 Is required for meiosis but not for mating type switching, end joining, or telomere maintenance. Mol. Cell. Biol. **19:**556–566.
46. **Moreau, S., E. A. Morgan, and L. S. Symington.** 2001. Overlapping Functions of the *Saccharomyces cerevisiae* Mre11, Exo1 and Rad27 Nucleases in DNA Metabolism. Genetics **159:**1423–1433.
47. **Mozlin, A. M., C. W. Fung, and L. S. Symington.** 2008. Role of the *Saccharomyces cerevisiae* Rad51 paralogs in sister chromatid recombination. Genetics **178:**113–126.
48. **Neale, M. J., J. Pan, and S. Keeney.** 2005. Endonucleolytic processing of covalent protein-linked DNA double-strand breaks. Nature **436:**1053–1057.
49. **Nicolette, M. L., et al.** 2010. Mre11-Rad50-Xrs2 and Sae2 promote 5′ strand resection of DNA double-strand breaks. Nat. Struct. Mol. Biol. **17:**1478–1485.
50. **Niu, H., et al.** 2010. Mechanism of the ATP-dependent DNA end-resection machinery from *Saccharomyces cerevisiae*. Nature **467:**108–111.
51. **Pace, P., et al.** 2010. Ku70 corrupts DNA repair in the absence of the Fanconi anemia pathway. Science **329:**219–223.

52. **Paillard, S., and F. Strauss.** 1991. Analysis of the mechanism of interaction of simian Ku protein with DNA. Nucleic Acids Res. **19:**5619–5624.
53. **Pang, D., S. Yoo, W. S. Dynan, M. Jung, and A. Dritschilo.** 1997. Ku proteins join DNA fragments as shown by atomic force microscopy. Cancer Res. **57:**1412–1415.
54. **Paull, T. T., and M. Gellert.** 1998. The 3′ to 5′ exonuclease activity of Mre 11 facilitates repair of DNA double-strand breaks. Mol. Cell **1:**969–979.
55. **Paulovich, A. G., and L. H. Hartwell.** 1995. A checkpoint regulates the rate of progression through S phase in *S. cerevisiae* in response to DNA damage. Cell **82:**841–847.
56. **Pommier, Y.** 2006. Topoisomerase I inhibitors: camptothecins and beyond. Nat. Rev. Cancer. **6:**789–802.
57. **Pommier, Y., et al.** 2006. Repair of topoisomerase I-mediated DNA damage. Prog. Nucleic Acid Res. Mol. Biol. **81:**179–229.
58. **Redon, C., et al.** 2003. Yeast histone 2A serine 129 is essential for the efficient repair of checkpoint-blind DNA damage. EMBO Rep. **4:**678–684.
59. **Seiler, J. A., C. Conti, A. Syed, M. I. Aladjem, and Y. Pommier.** 2007. The intra-S-phase checkpoint affects both DNA replication initiation and elongation: single-cell and -DNA fiber analyses. Mol. Cell. Biol. **27:**5806–5818.
60. **Shim, E. Y., et al.** 2010. *Saccharomyces cerevisiae* Mre11/Rad50/Xrs2 and Ku proteins regulate association of Exo1 and Dna2 with DNA breaks. EMBO J. **29:**3370–3380.
61. **Tomita, K., et al.** 2003. Competition between the Rad50 complex and the Ku heterodimer reveals a role for Exo1 in processing double-strand breaks but not telomeres. Mol. Cell. Biol. **23:**5186–5197.
62. **Tran, P. T., N. Erdeniz, S. Dudley, and R. M. Liskay.** 2002. Characterization of nuclease-dependent functions of Exo1p in *Saccharomyces cerevisiae*. DNA Repair (Amst.) **1:**895–912.
63. **Trujillo, K. M., and P. Sung.** 2001. DNA structure-specific nuclease activities in the *Saccharomyces cerevisiae* Rad50*Mre11 complex. J. Biol. Chem. **276:**35458–35464.
64. **Trujillo, K. M., S.-S. Yuan, E. Y. Lee, and P. Sung.** 1998. Nuclease activities in a complex of human recombination and DNA repair factors Rad50, Mre11, and p95. J. Biol. Chem. **273:**21447–21450.
65. **Usui, T., H. Ogawa, and J. H. Petrini.** 2001. A DNA damage response pathway controlled by Tel1 and the Mre11 complex. Mol. Cell **7:**1255–1266.
66. **Usui, T., et al.** 1998. Complex formation and functional versatility of Mre11 of budding yeast in recombination. Cell **95:**705–716.
67. **Vance, J. R., and T. E. Wilson.** 2002. Yeast Tdp1 and Rad1-Rad10 function as redundant pathways for repairing Top1 replicative damage. Proc. Natl. Acad. Sci. U. S. A. **99:**13669–13674.
68. **Wasko, B. M., C. L. Holland, M. A. Resnick, and L. K. Lewis.** 2009. Inhibition of DNA double-strand break repair by the Ku heterodimer in mrx mutants of *Saccharomyces cerevisiae*. DNA Repair (Amst.) **8:**162–169.
69. **Williams, R. S., et al.** 2008. Mre11 dimers coordinate DNA end bridging and nuclease processing in double-strand-break repair. Cell **135:**97–109.
70. **Yu, J., K. Marshall, M. Yamaguchi, J. E. Haber, and C. F. Weil.** 2004. Microhomology-dependent end joining and repair of transposon-induced DNA hairpins by host factors in *Saccharomyces cerevisiae*. Mol. Cell. Biol. **24:**1351–1364.
71. **Zhang, Y., et al.** 2007. Role of Dnl4-Lif1 in nonhomologous end-joining repair complex assembly and suppression of homologous recombination. Nat. Struct. Mol. Biol. **14:**639–646.
72. **Zhu, Z., W. H. Chung, E. Y. Shim, S. E. Lee, and G. Ira.** 2008. Sgs1 helicase and two nucleases Dna2 and Exo1 resect DNA double-strand break ends. Cell **134:**981–994.